Fault Ride-Through Performance of Electrolyzers with Partial Load and Ramp Rate Limitations

Manuel Agredano-Torres
KTH Royal Institute of Technology
Stockholm, Sweden
manuelat@kth.se

Ridma Wijethunga
Monash University
Melbourne, Australia
wijethunga.wijethunga@monash.edu

Supun Meetiyagoda
Monash University
Melbourne, Australia
supun.meetiyagoda@monash.edu

Behrooz Bahrani
Monash University
Melbourne, Australia
behrooz.bahrani@monash.edu

Mehdi Ghazavi Dozein
Monash University
Melbourne, Australia
mehdi.ghazavidozein@monash.edu

Qianwen Xu
KTH Royal Institute of Technology
Stockholm, Sweden
qianwenx@kth.se

***Abstract*—There is an ongoing discussion on how large inverter-based loads (IBLs), such as hydrogen electrolysis plants, should behave during faulty conditions and what their actual Fault Ride-Through (FRT) capabilities are. To enhance system stability and prevent sudden unexpected load disconnections, system operators are imposing FRT requirements on IBLs. In the context of large-scale electrolyzers, the hydrogen plant comprises multiple controllers and internal components, each with operational limits that may influence the overall plant performance during faulty conditions. This paper proposes an electrolyzer model with FRT strategy that reduces electrolyzer active power consumption to maximize reactive power support during faults, consistent with the latest grid-code requirements. More importantly, we demonstrate how inherent physical constraints, such as partial load limit and ramp rate limit, may prevent electrolyzers from meeting specific FRT requirements. This reveals a critical gap in current grid-code requirements, which largely overlook these technology-specific limitations. In addition, we explore potential technological solutions to improve electrolyzer FRT performance, including the use of supercapacitors integrated into the plant DC-link. The efficacy of the proposed electrolyzer model for FRT studies, including the identified FRT challenges and the proposed supercapacitor-based solution, is evaluated on a 5-MW electrolysis system.**

***Index Terms*—Large Inverter-based Loads, Fault Ride-through Operation, Electrolyzer, Ramp rate Limit, Partial Load Limit**

I. Introduction

Hydrogen is a key energy carrier for the decarbonization of hard-to-abate sectors, such as steel industry, and several industry applications such as transport [1], [2]. Green hydrogen is produced using electrolyzers supplied by renewable energy resources. Electrolyzers are devices interfaced with the grid via power-electronics inverters, that decompose water into hydrogen and oxygen with the use of electric power. There is a rapid growth in the grid integration of electrolysis plants, with global installed capacity rising from 0.6 GW in 2021 to 4.9 GW in 2025, and projected to reach 439 GW by 2030 [3]. In Sweden, the Transmission System Operator (TSO) estimates that hydrogen production will account for one-third of national electricity use by 2045 [4].

The nominal capacity of large-scale hydrogen electrolysis plants is expected to be in the order of MWs up to a few GWs in the near future [3], [5]. Considering the size of these systems, the sudden disconnection of electrolyzers can potentially cause a significant power imbalance in the grid, posing stability challenges to power systems, particularly under low-inertia and weak grid connections. Several TSOs have started working on grid requirements for large inverter-based loads (IBLs) such as electrolyzers and data centres [6], [7]. German TSOs have proposed grid-code requirements for large-scale electrolysis plants, with a key focus on Fault Ride-Through (FRT) requirements to avoid their sudden disconnection during faults [8]. For sudden voltage changes from 110% to 130% or lower than 90%, electrolyzers need to remain connected for at least 0.1 s or more depending on the voltage level. If possible, reactive power injection should be prioritized and active power consumption must be reduced. In addition, the active power recovery after the fault should be achieved in less than 1 s. However, it is not clear how and to what extent such sudden changes in active power consumption of electrolysis stacks is feasible, given certain operational limitations on electrolysis stacks such as ramp rate [10] and partial load limits [12].

The flexible operation and dynamic behavior of electrolyzers have been studied in the literature. In [9], the authors investigate the electrolyzer capabilities in providing frequency control services while considering ramp rate limitations on active power consumption. Similar study is presented in [10] considering both alkaline and proton exchange membrane (PEM) technologies. In [11], the authors investigate grid balancing services from electrolyzers in the context of offshore energy hubs, with a focus on ramp rate limitation effects on electrolyzer flexible operation. In [12], the authors study frequency and voltage support services from electrolyzers while considering partial load limitations in electrolysis plants. What is still lacking is clarity on the *actual* FRT capabilities

This work is supported by the Swedish strategic research programme StandUp for Energy, and the Swedish Energy Agency, Project No. 52650-1: Using hydrogen electrolyzer power electronics to balance high share of wind power.

979-8-3315-8138-1

of electrolysis plants and the challenges that may impede their ability to satisfy certain grid-code requirements. In this regard, only a few studies have examined the FRT behavior of electrolyzers. For example, both [13] and [14] study the electrolyzer performance under faulty conditions, but neither incorporates operational constraints, e.g., partial load or ramp rate limits, into their FRT models. The authors in [15] consider stack partial load limit in FRT studies, ignoring the ramp rate limitations on active power consumption. Accordingly, the literature lacks studies that analyze electrolyzer FRT performance and modelling considering stack operational constraints (partial load and ramp rate limits). This gap underscores the novelty of the work presented in this paper. The contributions and novelty of the work are thus summarized below:

1) Presenting an electrolyzer dynamic model for FRT studies, that incorporates its power-electronics interface, active/reactive power prioritization strategy, and stack constraints such as partial load and ramp rate limits;
2) Highlighting the technical challenges in FRT operation of electrolysis plants, those related to partial load and ramp rate limits, considering various system faults (near-zero, low, and high impedance faults);
3) Investigating possible technological solutions to enhance electrolyzer FRT performance, particularly supercapacitor integration into electrolysis plants.

The rest of the paper is organized as follows: Section II reviews the main electrolysis technologies and their operation limits. Section III introduces the electrolyzer model used for FRT analysis, incorporating operational limits. Section IV presents simulation case studies evaluating the FRT performance of the electrolyzer and a supercapacitor-based enhancement solution, while Section V presents the conclusions.

II. Electrolysis Technologies and Stack Operational Limitations Impacting FRT Operation

Alkaline and PEM electrolyzers are the two main technologies for large-scale applications [5]. For both alkaline and PEM electrolyzers, Fig. 1 shows a generalized electrical model without considering operational limitations such as partial load and ramp rate limitations [18]. The capacitances, C^a_{EDL} and C^c_{EDL}, represent the accumulated charge in the Electric Double Layer (EDL) between the electrodes (i.e., anode and cathode) and the electrolyte [16], [17]. The Charge Transfer (CT) losses in this interface are represented by the resistances, R^a_{CT} and R^c_{CT}. R_i represents the internal ohmic losses in electrolyte and electrical connections. V_{ref} is the minimum voltage required to start the hydrogen production.

Table I presents certain technical parameters of alkaline and PEM electrolyzers relevant to FRT operation [5], [10], [12]. It is not appropriate to require electrolysis plants to perform FRT operation during start-up and shutdown due to the specific procedures involved. It is especially relevant when these procedures last more than several seconds, such as in the cold start-up of PEM electrolyzers or warm start-up of alkaline electrolyzers, as per Table I.

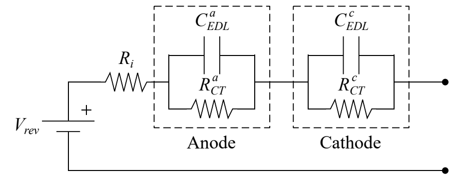

Fig. 1. Generalized electrolyzer model, without considering stack operational limitations.

TABLE I
Technical parameters of large-scale electrolyzers relevant to FRT operation [5], [10], [12].

Parameter	Alkaline electrolyzer	PEM electrolyzer
Cold start time	1 − 2 hours	1 − 5 minutes
Warm start time	5 − 10 minutes	Few seconds
Partial load limit	10% − 40%	0% − 10%
Ramp rate limit	0.2%/s − 20%/s	10%/s − 100%/s

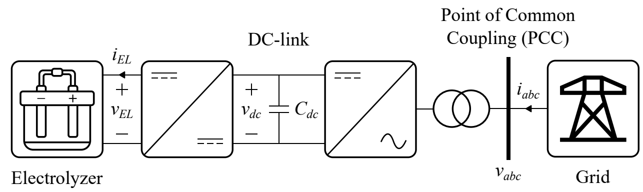

Fig. 2. Overall sketch of the electrolysis plant model considered in this study.

The partial load limit is relevant to the FRT operation since it defines the minimum active power level that electrolyzers can sustain while in operation. Since this limit is typically non-zero (as per Table I), electrolyzers should not reduce their active power to zero, as required by most FRT requirements defined by system operators. While electrolyzers operating below their partial load threshold may withstand infrequent total power outages, this does not apply to regular ride-through behavior expectations.

Ramp rate limit is another operational constraint relevant to the FRT operation. This is since the ramp rate limit determines the maximum available range for an electrolyzer to ramp up/down its power consumption over a period of time. Electrolyzers with stringent ramp rate limitations are not able to respond quickly enough to satisfy FRT requirements demanding fast active power reduction and recovery.

III. Proposed Electrolyzer Dynamic Model with Operational Constraints Suitable for FRT Studies

As shown in Fig. 2, a large-scale electrolyzer is connected to the grid at the Point of Common Coupling (PCC) through a two-stage power-electronics interface. The AC grid voltage is stepped down by a transformer and converted to DC voltage via an AC-DC converter. This grid-side converter is modeled as a three-phase active rectifier. The DC-link capacitor is placed between the AC-DC converter and a DC-DC converter which is connected to the electrolysis stack. This stack-side converter is modeled as a buck power converter.

979-8-3315-8138-1

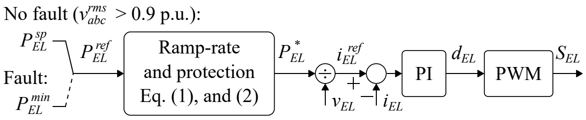

Fig. 3. Proposed stack-side converter control considering partial load limit and ramp rate limit of electrolysis stack.

The proposed stack-side converter control is shown in Fig. 3 considering the ramp rate and partial load limits, as well as a power consumption reduction strategy under faulty conditions. In normal conditions, the electrolyzer power reference P_{EL}^{ref} is equal to the electrolyzer set point P_{EL}^{sp} with no ramp rate and partial load limits. To maximize the reactive power support of the grid-side converter as requested by most recent grid codes, the power consumption of the electrolyzer must be reduced in faulty conditions. Therefore, in the case of a fault with the Root Mean Square (RMS) level of the grid voltage v_{abc}^{rms} lower than 0.9 in per unit (p.u.), P_{EL}^{ref} is determined by the partial load limit of P_{EL}^{min}. If the electrolyzer has a ramp rate limit K_r in [%/s], P_{EL}^{ref} is also modified to P_{EL}^{*} considering:

$$P_{EL}^{*} = \begin{cases} P_{EL}^{0} + K_r P_{EL}^{R} t & \text{if } P_{EL}^{*} < P_{EL}^{ref} \\ P_{EL}^{ref} & \text{if } P_{EL}^{*} = P_{EL}^{ref} \\ P_{EL}^{0} - K_r P_{EL}^{R} t & \text{if } P_{EL}^{*} > P_{EL}^{ref} \end{cases} \quad (1)$$

where t is the time duration since P_{EL}^{ref} changes from its initial value P_{EL}^{0}, and P_{EL}^{R} is the rated electrolyzer power. For further electrolyzer protection, the power reference P_{EL}^{*} is compared to the measured stack power, and the electrolyzer is disconnected if there is a mismatch higher than a certain tolerance tol:

$$P_{EL}^{*} = 0 \quad \text{if } |P_{EL}^{*} - v_{EL} i_{EL}| > tol \quad (2)$$

where v_{EL} and i_{EL} are the measured electrolyzer voltage and current. Once P_{EL}^{*} is calculated, it is divided by v_{EL} to obtain the current reference i_{EL}^{ref}. The difference between the current reference and measurement is used as an input for a PI controller to obtain the duty cycle d_{EL} of the stack-side converter, which is transformed to the switching signal S_{EL} by Pulse Width Modulation (PWM).

The grid-side converter is responsible for providing reactive power support to the grid, as well as DC-link voltage control. Its control strategy is shown in Fig. 4. A droop control with gain K_Q calculates reactive power reference Q^{ref}:

$$Q^{ref} = K_Q (v_{abc}^{rms} - v_{rms}^{ref}) \quad (3)$$

where v_{rms}^{ref} is the reference of the grid voltage v_{abc}^{rms}. The control of the DC-link voltage is a function of the power balance in the DC-link capacitor. The grid-side converter active power P depends on the energy stored in the DC-link capacitor and the power supplied to the electrolyzer P_{EL}:

$$P = C_{dc} \frac{d}{dt} \left(\frac{v_{dc}^2}{2} \right) + P_{EL} \quad (4)$$

where C_{dc} is the DC-link capacitance value, and v_{dc} is the DC-link voltage. Over-sizing the DC-link capacitor may thus

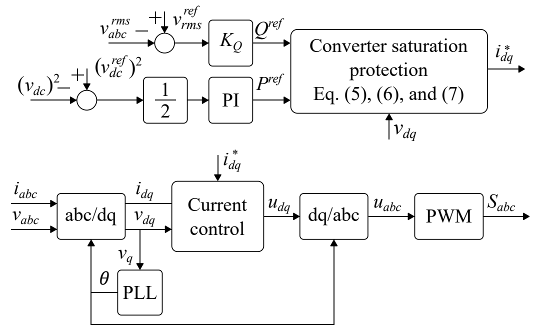

Fig. 4. Proposed grid-side converter control scheme for FRT operation considering power prioritization.

help with DC-link voltage control, which will be studied in simulation case studies. Therefore, the active power reference P^{ref} is calculated with a Proportional-Integral (PI) controller, considering the square value of v_{dc} and its reference v_{dc}^{ref}.

P^{ref} and Q^{ref} are translated to current references for the current control. This transformation is performed by the instantaneous power theory [19]:

$$\begin{bmatrix} i_d^{ref} \\ i_q^{ref} \end{bmatrix} = \frac{1}{v_d^2 + v_q^2} \begin{bmatrix} v_d & v_q \\ v_q & -v_d \end{bmatrix} \begin{bmatrix} P^{ref} \\ Q^{ref} \end{bmatrix} \quad (5)$$

where i_{dq}^{ref} is the current reference in dq coordinates, without consideration of converter saturation. As dq coordinates are synchronized with v_q and this component tends to zero, i_d^{ref} is approximately directly related to P^{ref}, and i_q^{ref} to Q^{ref}.

In the case of severe system faults (e.g., short-circuit faults), the PCC voltage drops sharply, and the current increases, leading to grid-side converter saturation. Under faulty conditions, the stack-side converter reduces its consumption down to the partial load limit to maximize the reactive power injection of the grid-side converter. However, the control of the DC-link voltage needs to be guaranteed to avoid the activation of the electrolyzer protection and its consequent disconnection. To ensure the DC-link voltage control, the current component directly related to active power i_d is allowed to reach the entire current saturation of the grid-side converter I_{sat}:

$$i_d^{*} = Min\left(i_d^{ref}, I_{sat}\right) \quad (6)$$

where i_d^{*} is the reference value of the d-axis current component after converter saturation. In the case of i_q^{*}, the reactive power injection is permitted provided that a sufficient inverter capacity remains available:

$$i_q^{*} = Min\left(i_q^{ref}, \sqrt{I_{sat}^2 - (i_d^{*})^2}\right). \quad (7)$$

The current reference i_{dq}^{*} is used in a standard current control for grid-side converters. For this control, the measured PCC current and voltage are transformed from stationary coordinates, i_{abc} and v_{abc}, to dq coordinates, i_{dq} and v_{dq}. A Phase-Locked Loop (PLL) is used to synchronize the dq coordinates to the q component. i_{dq} and v_{dq} are used in the current control to follow the current reference i_{dq}^{*}. The current

979-8-3315-8138-1

TABLE II
PARAMETERS OF THE SYSTEM UNDER STUDY.

Parameter	Value
Grid Thevenin voltage	11 kV
Grid Thevenin inductance	750 μH
Grid Thevenin resistance	34 mΩ
Transformer voltage at low-voltage side	0.4 kV
Power-electronics interface rated power	5 MW
Power-electronics interface saturation current	1.2 p.u.
Reactive power droop gain K_Q	5 p.u.
Grid-side filter inductance	30 μH
Grid-side filter resistance	0.1 mΩ
Rated DC-link voltage	1 kV
DC-link capacitance C_{dc}	0.2 F
Rated electrolyzer voltage	670 V
Rated electrolyzer power P_{EL}^R	5 MW
Electrolyzer protection tolerance *tol*	0.03 p.u.
Stack-side filter inductance	2 mH

control obtains the input voltage signal of the rectifier u_{dq}. This signal is transformed back to stationary coordinates u_{abc}, and is converted to the switching signals S_{abc} through PWM.

IV. SIMULATION CASE STUDIES

Electromagnetic Transient (EMT) simulations are performed to assess how electrolyzer operational limits affect its FRT performance, using a 5-MW electrolysis unit experiencing a three-phase fault at the PCC. The parameters of the electrolyzer stack model without operational limits (i.e., the model shown in Fig. 1) are derived from [18], and the PI controllers are designed according to the method presented in [20]. Other parameters of the electrolysis system under study are shown in Table II. For the presented case studies, the FRT requirement is defined as the ability to maintain the electrolyzer connected during 5 frequency cycles (0.1 s) with a near-zero fault impedance condition (i.e., v_{abs}^{rms}= 0 p.u.).

A. FRT Performance of Electrolyzers with Operational Limits

Fig. 5 shows the response of the system under different electrolyzer operational limits for near-zero impedance, low impedance, and high impedance fault conditions. The three-phase fault occurs at the PCC and lasts for five frequency cycles (0.1 sec) before the fault clearance. When there is no operational limits on the electrolysis plant, the electrolyzer remains connected under all faulty conditions. This is due to its rapid ability to reduce active power to zero during the fault, which keeps the DC bus voltage within a safe range (See Fig. 5, where the DC-link voltage stays above 0.8 kV in all simulation scenarios with no operational constraints). The key distinction among the three simulation scenarios with different fault impedance values is that a higher fault impedance Z_f results in a higher PCC voltage v_{abc}^{rms}, allowing the grid-side converter to supply more reactive power to the grid.

When the partial load limit P_{min} is considered and set to 40 % of the electrolyzer rated power (i.e., P_{min}=2 MW), as of the real-life example presented in Table I, the electrolyzer is disconnected under near-zero (Z_f=0.001 Ω) and low fault impedance (Z_f=0.05 Ω) simulation scenarios. In these two

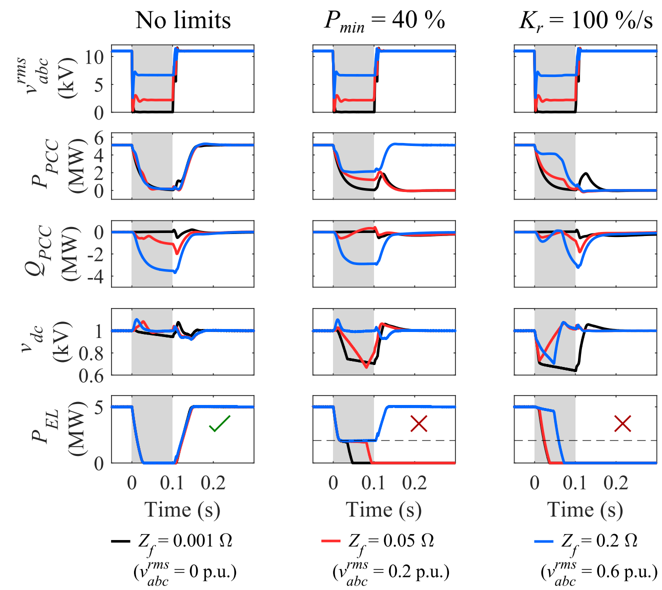

Fig. 5. FRT simulation studies of 5 MW electrolyzer considering different scenarios with various fault impedance values and electrolyzer operational limitations.

scenarios, the DC-link voltage drops sharply and is not able to maintain the power of the electrolyzer above the partial load limit of 2 MW. The DC-link voltage drop relates to the imbalance between the active power obtained from the grid-side converter and the power consumed by the electrolyzer.

Electrolyzer inability in FRT operation also occurs when the highest ramp rate of 100 %/s (i.e., 5 MW/s), as per Table I, is considered. This case is more severe, as the power consumption of the electrolyzer remains at higher levels during the fault, causing the disconnection of the electrolyzer even under high fault impedance conditions. The disconnection of the electrolyzer implies that the system is not able to withstand the fault and provide FRT performance as required by the current grid-code requirements [8].

B. FRT Performance Enhancement by Supercapacitor

The DC-link capacitor can be over-sized with a supercapacitor to achieve a slow change in the DC-link voltage. Even the highest ramp-rate limit in Table I (K_r = 100%/s) only reduces the electrolyzer power to 90% during a 0.1 s fault. Therefore, the conservative case of constant electrolyzer consumption at P_{EL}^R is considered for the supercapacitor sizing. A simple back-of-the-envelope sizing expression can be obtained considering that the capacitor must be able to supply at least the consumed energy by the electrolyzer:

$$C_{dc}\frac{V_0^2 - V_{\text{min}}^2}{2} \geq P_{EL}^R\ t_{\text{fault}} \ \Rightarrow\ C_{dc} \geq \frac{2P_{EL}^R t_{\text{fault}}}{V_0^2 - V_{\text{min}}^2} \quad (8)$$

where V_0 is the initial capacitor voltage, V_{min} is permissible minimum voltage, and t_{fault} is the fault duration.

The capacitance is increased by one order of magnitude, from 0.2 F to 2 F, considering V_0 is equal to the rated DC-link voltage and V_{min} is equal to 0.7 kV. Fig. 6 shows the

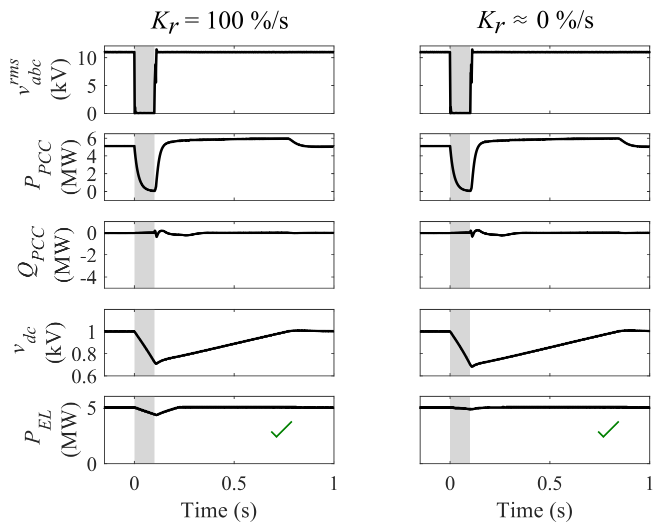

Fig. 6. Simulation results of the 5 MW electrolysis system with a supercapacitor, under near-zero fault impedance conditions with Z_f equal to 0.001 Ω (v_{abs}^{rms}= 0 p.u.) and different stack ramp rates.

response of the electrolyzer system for the worst-case scenario of Fig. 5 ($Z_f = 0.001$ Ω and $K_r = 100$ %/s), and a more conservative case of K_r close to 0 %/s. In both cases, the supercapacitor helps limit the DC-link voltage dip, keeping it around 0.7 kV (Fig. 5), thereby improving the electrolyzer FRT performance and preventing its disconnection. However, this benefit comes at a cost, as the post-fault voltage recovery time is also noticeably extended. Therefore, the electrolyzer is able to fulfill the FRT requirements and remain connected, avoiding grid power imbalances following the fault clearance. However, there is an increase in the cost of the system due to the DC bus capacitance size increase, as well as a slower recovery of the DC bus voltage. So, a techno-economic assessment is required to investigate further the feasibility of a supercapacitor solution.

V. Conclusion

This paper evaluates the Fault Ride-Through (FRT) performance of electrolyzers with partial load and ramp rate limits, using EMT simulations. The findings show that the electrolyzer can successfully remain connected during severe grid faults when there is no operational limits on the stack. However, once realistic constraints, such as minimum partial load and ramp rate limits, are introduced, its ability to ride through faults is significantly reduced. In particular, ramp rate limitation makes the electrolyzer unable to stay connected under any of the faulty conditions studied in this paper. Therefore, extra investments are required to enhance the FRT performance of the electrolysis plant. The integration of supercapacitor into the DC bus has been explored as possible solution. This has proved effective in slowing the DC-link voltage drop and restoring FRT capability even under stringent ramp rate limits. This solution, however, introduces trade-offs, including a slower post-fault voltage recovery and potential economic challenges. Future work aims to study these challenges, as well as other possible solutions, such as oversizing the grid-side converter to increase the saturation current level, or the use of battery storage. Furthermore, the FRT performance of electrolyzers under unbalanced faulty conditions should also be studied.

References

[1] L. A. Lambert et al., "The EU's natural gas Cold War and diversification challenges," *Energy Strategy Reviews*, vol. 43, pp. 100934, Sep. 2022.

[2] Fuel Cells and Hydrogen 2 Joint Undertaking "Increasing Electric Power System Flexibility: The Role of Industrial Electrification and Green Hydrogen Production," Energy Systems Integration Group ESIG, Reston, VA, USA, Tech. Rep., 2019.

[3] 'International Energy Agency, 'Global Hydrogen Review 2025," IAE, Paris, France, Tech. Rep., 2024.

[4] M. Jonsson, K. Brunge, E. Hellström, M. Jakobsson, and E. Thornberg, "Långsiktig marknadsanalys 2021 Scenarier för elsystemets utveckling fram till 2050," Svenska Kraftnät, Sundbyberg, Sweden, Tech. Rep., 2019.

[5] Flexibility Resources Task Force "Increasing Electric Power System Flexibility: The Role of Industrial Electrification and Green Hydrogen Production," Energy Systems Integration Group ESIG, Reston, VA, USA, Tech. Rep., 2022.

[6] D. Baker, M. Sedighizadeh, "High impact large load ride-through requirements," Southwest Power Pool SPP, Little Rock, AR, USA, Tech. Rep., 2025.

[7] Alberta Electric System Operator, "AESO Connection Requirements for Transmission-Connected Data Centres," AESO, Calgary, Canada, Tech. Rep., 2025.

[8] Netztransparenz, "Technical requirements for the connection of electrolyser facilities," netztransparenz, Netztransparenz, Germany, Tech. Rep., 2024.

[9] B. W. Tuinema, E. Adabi, P. K. S. Ayivor, V. Garcia Suarez, L. Liu, A. Perilla et al., "Modelling of large-sized electrolysers for real-time simulation and study of the possibility of frequency support by electrolysers," *IET Gener. Transm. Distrib.*, vol. 14, no. 10, pp. 1985–1992, May 2020.

[10] N. Taranin, M. G. Dozein, O. Saborio-Romano and N. A. Cutululis, "On the Ramp-Rate Limitation of Electrolysis Plants: Modeling Fundamentals and System-Level Impact Analysis," *IEEE Transactions on Sustainable Energy*, Early Access, 2025.

[11] N. Taranin, T. Grimsdottir, D. Müller, M. Nuhic, G. F. Gontijo and N. A. Cutululis, "Power Balancing Services from Electrolyzer on Offshore Energy Hub," *2025 IEEE Kiel PowerTech*, Kiel, Germany, 2025.

[12] S. H. Meetiyagoda, B. Bahrani and M. G. Dozein, "Distribution-Connected Electrolyzers with Partial Loading Limit and Power Response Characteristics," *2025 IEEE Kiel PowerTech*, Kiel, Germany, 2025.

[13] S. D. Tavakoli et al., "Grid-Forming Services From Hydrogen Electrolyzers," *IEEE Transactions on Sustainable Energy*, vol. 14, no. 4, pp. 2205-2219, Oct. 2023.

[14] N. Wiese, D. Ghosh, P. Kretschmer, S. Eberlein and D. Strauß-Mincu, "Grid-Forming Controlled Electrolyzer with LVRT Capability and Asymmetric Inertia Provision," *2024 International Conference on Smart Energy Systems and Technologies (SEST)*, Torino, Italy, 2024.

[15] X. Shen, Y. Li, C. Shen, Y. Shen and H. Liu, "2025 IEEE 8th International Electrical and Energy Conference (CIEEC)," *2025 IEEE Kiel PowerTech*, Changsha, China, 2025.

[16] T. Smolinka, E. T. Ojong, and J. Garche, "Hydrogen Production from Renewable Energies-Electrolyzer Technologies," *Electrochemical Energy Storage for Renewable Sources and Grid Balancing*,pp. 103–128. Oxford, UK: Elsevier, 2015.

[17] T. F. Fuller, and J. N. Harb, *Electrochemical Engineering*, 1st ed., John Wiley & Sons, New Jersey, USA, 2018

[18] F. W. Speckmann, S. Bintz, M. L. Groninger, and K. P. Birke, "Alkaline Electrolysis with Overpotential-Reducing Current Profiles," *ECS Transactions*, vol. 83, no. 1, pp. 179-194, 2018.

[19] H. Akagi, E. H. Watanabe, and M. Aredes, *Instantaneous Power Theory and Applications to Power Conditioning*, John Wiley & Sons, New Jersey, USA, 2007.

[20] S. Bacha, I. Munteanu, A. Bratcu, "General Control Principles of Power Electronic Converters," in *Power Electronic Converters Modeling and Control*, Springer, London, UK, 2014.

979-8-3315-8138-1